FLUX-SPLITTING SCHEMES FOR IMPROVED MONOTONICITY OF DISCRETE SOLUTIONS OF ELLIPTIC EQUATIONS WITH HIGHLY ANISOTROPIC COEFFICIENTS

Mayur Pal and Michael G. Edwards

Civil and Computational Engineering Centre, University of Wales Swansea
Singleton Park Swansea SA28PP, Wales-UK
e-mail: 339620@swansea.ac.uk

Key words: Family of flux-continuous schemes, monotonicity, maximum principle, anisotropy and pressure equation

Abstract. *A family of flux-continuous, locally conservative, finite-volume schemes has been developed for solving the general tensor pressure equation of petroleum reservoir-simulation on structured and unstructured grids. These schemes are control-volume distributed. The schemes are applicable to diagonal and full tensor pressure equation with generally discontinuous coefficients and remove the O(1) errors introduced by standard reservoir simulation schemes when applied to full tensor flow approximation. The family of flux-continuous schemes is quantified by a quadrature parameterization. Improved convergence using the quadrature parameterization has been established for the family of flux-continuous schemes.*

When applying these schemes to strongly anisotropic heterogeneous media they can fail to satisfy a maximum principle (as with other FEM and finite-volume methods) and result in loss of solution monotonicity for high anisotropy ratios causing spurious oscillations in the numerical pressure solution. This paper investigates the use of flux-splitting techniques to solve the discrete system for the problems with high anisotropy ratios and improve monotonicity of the solution. Flux-splitting schemes are presented together with a series of numerical results for test-cases with strong anisotropy ratios. In all cases the resulting numerical pressure solutions are free of spurious oscillations.

1 INTRODUCTION

Subsurface reservoirs generally have a complex description in terms of both geometry and geology. Rapid variation in permeability with strong anisotropy is common in reservoir simulation. Continuous flux and pressure discretization of the reservoir simulation pressure equation is required in order to honour correct local physical interface conditions between grid blocks, with strong discontinuities and anisotropy in permeabilities. The

derivation of algebraic flux continuity conditions for full tensor discretization operators has lead to efficient and robust locally conservative flux-continuous control volume distributed (CVD) finite-volume schemes for determining the discrete pressure and velocity fields in subsurface reservoirs[1,2,3,4,5,6,7,8]. Schemes of this type are also called as multi-point flux approximation schemes or MPFA[9,10,11,12,13]. Further schemes of this type are presented in[14,15,16]. All of these schemes are applicable to the diagonal and full tensor pressure equation with generally discontinuous coefficients and remove the O(1) error introduced by standard reservoir simulation schemes when applied to full tensor flow approximation. Other schemes that preserve flux continuity have also been developed using mixed methods[17] and discontinuous galerkin methods[18,19,20].

Monotonicity behavior of the family of flux-continuous schemes has been in question since its early formulation. Conditions for a symmetric positive definite matrix and diagonal dominance of the resulting discrete matrix for the family of schemes are presented in [1,2]. The discretization matrices obtained for the family of schemes in the case of a full tensor are conditionally diagonally dominant and not generally M-matrices[1]. For high anisotropic ratios with grid skewness the resulting discrete matrix for these schemes is found to be non-monotonic (as with more standard methods) and the numerical solution consequently exhibits spurious oscillations.

The aim of this paper is to address the monotonicity problem encountered in reservoir simulation and obtain a solution to this problem. The strategy presented here involves the use of flux-splitting introduced in[5] applied to the family of flux-continuous schemes. Properties of the flux-splitting schemes for the single-phase pressure equation are presented in [5,21]. Here it is shown that careful use of flux-splitting can remove the spurious oscillations introduced in the numerical pressure solution by highly anisotropic permeability tensors in porous medium. Previous work aimed at preserving monotonic behavior of the solutions for strong heterogeneity and skew grids is presented in[22]. Conditions for monotonicity have previously been derived in[1] for an M-matrix and in[23] for a monotone matrix. Grid optimization techniques have also been used to improve monotonicity of the discrete system[24]. However these techniques appear to be limited subject to permeability anisotropy ratio. In contrast, the flux-splitting techniques presented here are easier to implement for both structured and unstructured grids and can handle very strong anisotropic heterogeneity.

This paper is organized as follows: Section 2 gives a description of the single phase flow problem encountered in reservoir simulation with respect to the general tensor pressure equation. In Section 3 the details of the formulation of the family of flux-continuous finite volume scheme with discretization in *physical* space is presented. Section 4 summarizes conditions required to obtain a monotonic solution and describes performance of the family of flux-continuous schemes with respect to monotonicity, with the help of numerical examples. Section 5 describes the flux splitting technique to solve the discrete system and

shows how it can be used to compute a monotonic solution for the family of flux-continuous schemes. Section 6 presents numerical examples that demonstrate the use of flux-splitting techniques for preserving monotonicity. Conclusions follow in section 7.

2 FLOW EQUATION AND PROBLEM DESCRIPTION

2.1 Cartesian tensor

The problem is to find the pressure ϕ satisfying

$$-\int_\Omega \nabla \bullet \mathbf{K}(x,y)\nabla\phi d\tau = \int_\Omega q d\tau = \mathbf{M} \tag{1}$$

over an arbitrary domain Ω, subjected to suitable (Neumann/Dirichlet) boundary conditions on boundary $\partial\Omega$. The right hand side term $\mathbf{M}$ represents a specified flow rate and $\nabla = (\partial_x, \partial_y)$. Matrix $\mathbf{K}$ can be a diagonal or full cartesian tensor with general form

$$\mathbf{K} = \begin{pmatrix} K_{11} & K_{12} \\ K_{12} & K_{22} \end{pmatrix} \tag{2}$$

The full tensor pressure equation is assumed to be *elliptic* such that

$$K_{12}^2 \leq K_{11}K_{22} \tag{3}$$

The tensor can be discontinuous across internal boundaries of Ω. The boundary conditions imposed here are Dirichlet and Neumann. For incompressible flow pressure is specified at atleast one point in the domain. For reservoir simulation, Neumann boundary conditions on $\partial\Omega$ requires zero flux on solid walls such that $(K\nabla\phi) \cdot \hat{n} = 0$, where $\hat{n}$ is the outward normal vector to $\partial\Omega$.

2.2 General tensor equation

The pressure equation is defined above with respect to the *physical* tensor in the initial classical Cartesian coordinate system. Now we proceed to a general curvilinear coordinate system that is defined with respect to a uniform dimensionless transform space with a (ξ, η) coordinate system. Choosing Ω_p to represent an arbitrary control volume comprised of surfaces that are tangential to constant (ξ, η) respectively, equation 1 is integrated over Ω_p via the Gauss divergence theorem to yield

$$-\oint_{\partial\Omega_p} (\mathbf{K}\nabla\Phi) \cdot \hat{\mathbf{n}} ds = \mathbf{M} \tag{4}$$

where $\partial\Omega_p$ is the boundary of Ω_p and $\hat{n}$ is the unit outward normal. Spatial derivatives are computed using

$$\phi_x = J(\phi, y)/J(x, y), \phi_y = J(x, \phi)/J(x, y), \tag{5}$$

where $J(x,y) = x_\xi y_\eta - x_\eta y_\xi$ is the Jacobian. Resolving the x,y components of velocity along the unit normals to the curvilinear coordinates (ξ, η), e.g., for $\xi = $ constant, $\hat{\mathbf{n}}ds = (y_\eta, -x_\eta)d\eta$ gives rise to the general tensor flux components

$$F = -\int (T_{11}\phi_\xi + T_{12}\phi_\eta)d\eta, \quad G = -\int (T_{12}\phi_\xi + T_{22}\phi_\eta)d\xi, \tag{6}$$

where general tensor $\mathbf{T}$ has elements defined by

$$
\begin{aligned}
T_{11} &= (K_{11}y_\eta^2 + K_{22}x_\eta^2 - 2K_{12}x_\eta y_\eta)/J, \\
T_{22} &= (K_{11}y_\xi^2 + K_{22}x_\xi - 2K_{12}x_\xi y_\xi)/J, \\
T_{12} &= (K_{12}(x_\xi y_\eta + x_\eta y_\xi) - (K_{11}y_\eta y_\xi + K_{22}x_\eta x_\xi))/J
\end{aligned} \tag{7}
$$

and the closed integral can be written as

$$\int\int_{\Omega_p} \frac{(\partial_\xi \tilde{F} + \partial_\eta \tilde{G})}{J} J d\xi d\eta = \triangle_\xi F + \triangle_\eta G = m \tag{8}$$

where e.g. $\triangle_\xi F$ is the difference in net flux with respect to ξ and $\tilde{F} = T_{11}\phi_\xi + T_{12}\phi_\eta$, $\tilde{G} = T_{12}\phi_\xi + T_{22}\phi_\eta$. Thus any scheme applicable to a full tensor also applies to non-K-Orthogonal grids. Note that $T_{11}, T_{22} \geq 0$ and ellipticity of $\mathbf{T}$ follows from equations 3 and 7. Full tensors can arise from upscaling, and orientation of grid and permeability field. For example by equation 7, a diagonal anisotropic Cartesian tensor leads to a full tensor on a curvilinear *orthogonal* grid.

3 FAMILY OF FLUX-CONTINUOUS FINITE VOLUME SCHEMES
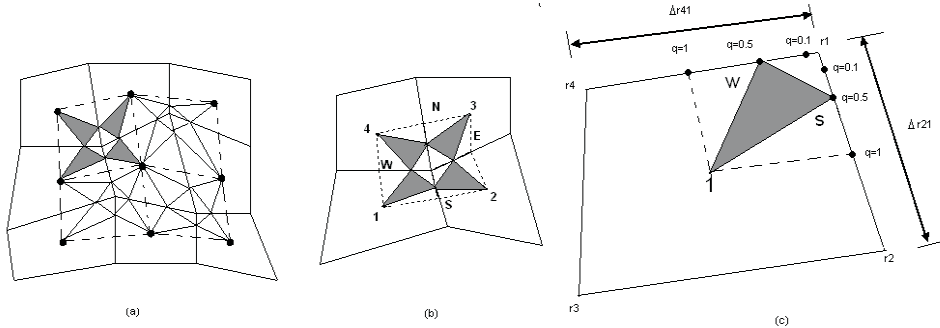
Figure 1: (a)Nine-point continuous pressure support, highlighted *dual-cell*. (b) Points of Flux-Continuity (N,S,E,W) on sub-cell faces of a *dual-cell* (c) Quadrature points on a sub-cell faces *q=0.1, q = 0.5 and q = 1*.

Families of flux-continuous locally conservative control-volume distributed (CVD) finite volume schemes presented in[1−8] have been developed for different grid types including cell

vertex structured and unstructured and cell centred formulations in physical space and transform space. Numerical convergence rates for a range of quadrature rules in physical space are presented in[7]. We present a summary here for structured the cell centred quadrilateral formulation, although results are presented for structured and unstructured grids. The nine node support of the scheme is indicated in figure 1(a)). The scheme has cell centred flow and rock variables, so that the approximation points (or nodes) are at the centres of the primal grid cells and the primal grid cells are also the control-volumes, i.e. CVD with respect to the primal grid cells. For each group of four nodes, four triangles are drawn as in figure 1(a). Each group is defined within a *dual-cell* which is obtained by joining cell centres with cell edge mid-points as indicated by the dashed contour in figure 1(b). The dual cells partition the primal cells (or control-volumes) into subcells[2]. Two faces of each subcell also define *sub faces* of two faces of the parent control-volume.

3.0.1 Family of Schemes - Quadrature parameterization

The family of schemes is formed when imposing normal flux and pressure continuity conditions on the *sub-faces* where the four shaded triangles meet, at the four positions (N, S, E, W), in (or on the perimeter of) the dual cell 1(b)). On each *sub-face* the point of continuity is parameterized with respect to the subcell by the variable q, where referring to figure 1(c) $(0 < q \leq 1]$. For a given subcell, the points of continuity can lie anywhere in the intervals $(0 < q \leq 1]$ on the two faces of each subcell inside a dual cell, that coincide with the control-volume *sub-faces*, and the value of q defines the quadrature point and hence the family of flux-continuous finite-volume schemes. The different values of quadrature point considered here are $q = 0.1, 0.5$ and 1 (figure 1(c)). Cell face pressures $\phi_N, \phi_E, \phi_S, \phi_W$ are introduced at N, S, E, W locations. Pressure sub-triangles are defined with local triangular support imposed within each quarter (sub-cell) of the *dual-cell* as shown in figure 1(b). Pressure ϕ, in local cell coordinates, is piecewise linear over each triangle. The *physical* space flux-continuity conditions for cells 1 to 4, sharing a common grid vertex inside the dual-cell are expressed as

$$
\begin{aligned}
F_N &= -\frac{1}{2}(T_{11}\phi_\xi + T_{12}\phi_\eta)|_N^3 = -\frac{1}{2}(T_{11}\phi_\xi + T_{12}\phi_\eta)|_N^4, \\
F_S &= -\frac{1}{2}(T_{11}\phi_\xi + T_{12}\phi_\eta)|_S^1 = -\frac{1}{2}(T_{11}\phi_\xi + T_{12}\phi_\eta)|_S^2, \\
F_E &= -\frac{1}{2}(T_{12}\phi_\xi + T_{22}\phi_\eta)|_E^2 = -\frac{1}{2}(T_{12}\phi_\xi + T_{22}\phi_\eta)|_E^3, \\
F_W &= -\frac{1}{2}(T_{12}\phi_\xi + T_{22}\phi_\eta)|_W^1 = -\frac{1}{2}(T_{12}\phi_\xi + T_{22}\phi_\eta)|_W^4
\end{aligned}
\tag{9}
$$

The above system of equations (9) is now expressed as

$$
F = A_L\Phi_f + B_L\Phi_v = A_R\Phi_f + B_R\Phi_v
\tag{10}
$$

where $F = (F_N, F_S, F_E, F_W)^T$ are the fluxes defined in the dual-cell and $\Phi_f = (\phi_N, \phi_S, \phi_E, \phi_W)^T$ are the interface pressures. Similarly $\Phi_v = (\phi_1, \phi_2, \phi_3, \phi_4)^T$ are the cell centered pressures. Thus the four interface pressures are expressed in terms of the four cell centered pressures. Using equation 10, Φ_f is now expressed in terms of Φ_v to obtain the dual-cell flux and coefficient matrix

$$F = (A_L(A_L - A_R)^{-1}(B_R - B_L) + B_L)\Phi_v \qquad (11)$$

Thus the cell-face pressures are eliminated from the flux by being determined locally in terms of the cell centered pressures in a preprocessing step, avoiding introduction of the interface pressure equations into the assembled discretization matrix. The equation 11 can also be written as

$$AF = -\Delta\Phi_v \qquad (12)$$

where the entries of matrix A are accumulated inverse tensor elements and $\Delta\Phi_v = (\phi_{21}, \phi_{32}, \phi_{34}, \phi_{41})^T$ are the differences of vertex pressures, see[2,6] for details. The physical space formulation does not posses a symmetric discretization matrix for arbitrary quadrilaterals, however transform space (cell and sub-cell) formulations that are symmetric positive definite are presented in[1,3,4,6]. Flux continuity in the case of a general-tensor is obtained while maintaining the standard single degree of freedom per cell. Since the continuity equations depend on both ϕ_ξ and ϕ_η (unless a diagonal tensor is assumed with cell-face midpoint quadrature resulting in a 2-point flux), the interface pressures $\Phi_f = (\phi_N, \phi_S, \phi_E, \phi_W)^T$ are locally coupled and each group of four interface pressures is determined simultaneously in terms of the group of four cell centered pressures whose union contains the continuity positions. Finally for a structured grid the scheme is defined by

$$F_{i+1/2,j} - F_{i-1/2,j} + F_{i,j+1/2} - F_{i,j-1/2} = M \qquad (13)$$

where i, j are the integer coordinates of the central quadrilateral cell, figure 1(a)) and

$$\begin{aligned}
F_{i+1/2,j} &= F_{S_{i+1/2,j+1/2}} + F_{N_{i+1/2,j-1/2}}, \\
F_{i,j+1/2} &= F_{E_{i-1/2,j+1/2}} + F_{W_{i+1/2,j+1/2}}
\end{aligned} \qquad (14)$$

where $i+1/2, j+1/2$ denote the "integer" coordinates of the top right hand side dual-cell, figure 1(a)). The unstructured formulation is presented in[2-5,7]

4 MONOTONICITY

The family of flux-continuous schemes results in a discrete matrix which forms 5-9 row entries in 2D and 7-27 row entries in 3D. The discrete system can be written as

$$\mathbf{A}\phi = b \qquad (15)$$

Where $\mathbf{A}$ is the discrete matrix operator, ϕ is the unknown pressure and b is the source term. Ideally the discrete system of equation 15 should be *monotone*, and satisfy a *maximum principle* that is analogous to that of the continuous counterpart of the discrete problem and hence ensuring that the numerical solution is free from nonphysical oscillations. The discrete matrix operator $\mathbf{A}$ is *monotone* if and only if $\mathbf{A}$ is non-singular and it obeys the following condition[25]

$$\mathbf{A^{-1}} \geq \mathbf{O} \tag{16}$$

where $\mathbf{O}$ is a zero matrix. While a monotone discretization matrix ensures that a non-negative source and boundary data yields a non-negative pressure field, it has not been proven that a monotone discretization matrix will prevent discrete spurious local extrema occuring in the discrete solution of the general tensor pressure equation. A sufficient condition for a maximum principle (which can ensure that no spurious extrema occur in the discrete solution) is that $\mathbf{A}$ is a $\mathbf{M-}$ matrix, i.e. monotone positive definite with $a_{i,j} \leq 0$. The following conditions (often easier to verify) also define an $\mathbf{M-}$ matrix:

$$
\begin{aligned}
a_{i,i} &> 0, \forall i \\
a_{i,j} &\leq 0, \forall i, j, i \neq j \\
\Sigma_j a_{i,j} &\geq 0, \forall i
\end{aligned} \tag{17}
$$

In addition $\mathbf{A}$ must either be strictly diagonally dominant,i.e.

$$A_{i,i} > \sum_{j=1, j \neq i}^{n} \mid A_{i,j} \mid, \quad i = 1, 2, ..., n \tag{18}$$

or else $\mathbf{A}$ must be irreducible and

$$A_{i,i} \geq \sum_{j=1, j \neq i}^{n} \mid A_{i,j} \mid, \quad i = 1, 2, ..., n \tag{19}$$

with strict inequality for at least one row. Conditions (derived in[1]) for nine-node flux continuous schemes to be an M-Matrix are

$$min(T_{1,1}, T_{2,2}) \geq \eta(q)(T_{1,1} + T_{2,2}) \geq T_{1,2} \tag{20}$$

where $\eta(q)$ is a function of quadrature point. One of the essential conditions here is that $T_{1,2} \leq min(T_{1,1}, T_{2,2})$, which is particularly limiting on the range of tensors that are applicable, so that in the general case these schemes do not possess M-Matrices.

We will now present numerical examples which demonstrate the loss of monotonicity and violation of maximum principle when using the finite volume formulation (note that standard schemes also fail on this example). In these examples a point source is introduced
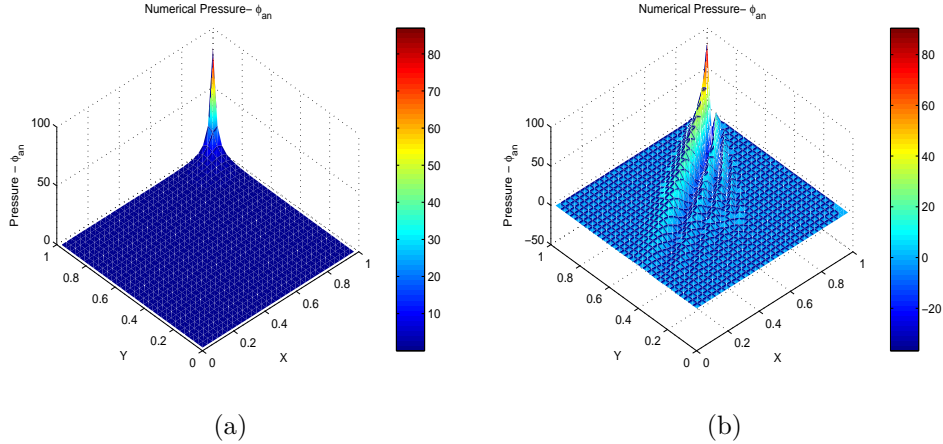
Figure 2: (a) Numerical Pressure solution with isotropic permeability tensor. (b) Numerical Pressure solution with Anisotropy ratio 1:1000 and angles between grid and principal permeability axes = 30 degrees.

at the corner of a square domain with orthogonal grid and zero Dirichlet pressure holds elsewhere on the boundary. Two different permeability tensor fields are tested and the results are shown in figure 2. It can be seen from figure 2(a) that the numerical pressure solution in the first case (isotropic) has a maximum principle. In the second case (with high anisotropy ratio, with grid *non-aligned* with the principal axes leading to a full-tensor) the tensor field violates Eq.20 and the numerical pressure solution shown in figure 2(b) clearly violates the maximum principle resulting in spurious oscillations with negative pressure, hence equation 16 is not valid in this case. The spurious oscillations in pressure do not disappear even with mesh refinement. A similar test with Green's function was presented in[23]. The violation of the maximum principle by the family of flux-continuous finite-volume schemes and standard CVFE for high anisotropy ratios presents a major challenge for numerical approximation of elliptic PDE's.

5 FLUX-SPLITTING TECHNIQUE

Flux-splitting for the family of flux-continuous finite volume schemes is presented in[5], where unconditional stability is proven for constant coefficients and its benefits were discussed with respect to computational efficiency. Further properties of flux-splitting discretization are also given in [5] where flux-splitting is defined so as to maintain local conservation at any iterative level, so that non-converged solutions are still locally conservative. A further study of iterative performance of flux-splitting is presented in[21]. In this section a brief overview of flux-splitting is presented and a modification is given to obtain monotonic solutions for cases with high anisotropy ratio. Following[5] fluxes are cast in the form of a leading two-point flux corresponding to the diagonal tensor together with cross-flow terms. The flux is now split so as to generate a semi-implicit scheme

that retains an implicit approximation of the diagonal tensor contribution and employs an explicit approximation of all flux cross-flow terms, thereby retaining standard diagonal tensor Jacobian inversion, and preserves existing simulator code design and efficiency.

5.1 Splitting at Matrix Level

First we consider splitting at matrix level. Let the fully implicit nine-point discretization matrix be denoted by $A^{(9)}$ and the discrete solution by ϕ_h. Now the matrix $A^{(9)}$ can be decomposed into a leading pentadiagonal matrix $A^{(5)}$ and a residual matrix $A^{(9-5)}$ where

$$A^{(9)} = A^{(5)} + A^{(9-5)} \tag{21}$$

the respective split matrices are denoted symbolically by

$$A^{(5)} = \begin{pmatrix} 0 & A^{(9)}_{i,j+1} & 0 \\ A^{(9)}_{i-1,j} & A^{(9)}_{i,j} & A^{(9)}_{i+1,j} \\ 0 & A^{(9)}_{i,j-1} & 0 \end{pmatrix} \tag{22}$$

$$A^{(9-5)} = \begin{pmatrix} A^{(9)}_{i-1,j+1} & 0 & A^{(9)}_{i+1,j+1} \\ 0 & 0 & 0 \\ A^{(9)}_{i-1,j-1} & 0 & A^{(9)}_{i+1,j-1} \end{pmatrix} \tag{23}$$

and give rise to a semi-implicit schemes of the form

$$A^{(5)}\phi^{n+1} + A^{(9-5)}\phi^n = b \tag{24}$$

5.2 Splitting at Flux level

The splitting is illustrated as follows: Let $\mathbf{A}$ denote the Jacobian matrix for the nine-point flux-continuous system of equations, and $\mathbf{B}$ denote the Jacobian matrix for the classical two-point system of equation. The basic principle behind flux splitting is to express the nine-point flux in terms of two-point flux evaluated at (iterate or time) level $(n+1)$ and a remainder term at level n, written as:

$$\mathbf{F^{NP}} = \mathbf{F^{TP^{n+1}}} + (\mathbf{F^{NP^n}} - \mathbf{F^{TP^n}}) \tag{25}$$

where $\mathbf{F^{NP}}$ is the consistent split-flux, NP is a 9-point operator in this case and TP is 2-point. First we rewrite the original discrete system of equations (Eq. 15) as:

$$\mathbf{B}\phi + (\mathbf{A} - \mathbf{B})\phi = b \tag{26}$$

where

$$B^{(5)} = \begin{pmatrix} 0 & B^{(5)}_{i,j+1} & 0 \\ B^{(5)}_{i-1,j} & B^{(9)}_{i,j} & B^{(5)}_{i+1,j} \\ 0 & B^{(5)}_{i,j-1} & 0 \end{pmatrix} \tag{27}$$

Transfinite Mesh 16x16

(a)   (b)
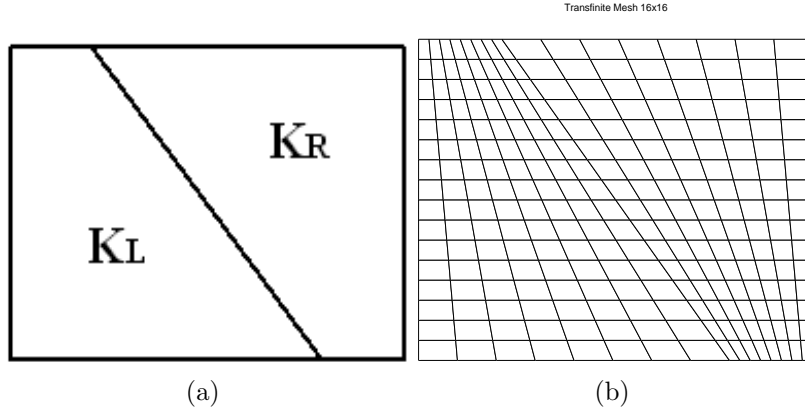
Figure 3: (a) Medium Discontinuity. (b) Mesh aligned along the discontinuity.

results from the 2-point flux and

$$
A^{(9)} - B^{(5)} = \begin{pmatrix} X^{(9)}_{i-1,j+1} & X^{(9)}_{i,j+1} & X^{(9)}_{i+11,j+1} \\ X^{(9)}_{i-1,j} & X^{(9)}_{i,j} & X^{(9)}_{i+1,j} \\ X^{(9)}_{i-1,j-1} & X^{(9)}_{i,j-1} & X^{(9)}_{i+1,j-1} \end{pmatrix} \tag{28}
$$

then the flux-split iteration is defined by:

$$
\mathbf{B}\phi^{k+1} = (\mathbf{B} - \mathbf{A})\phi^k + b \tag{29}
$$

The above equation results in the following iterative method:

$$
\phi^{k+1} = (\mathbf{I} - \mathbf{B^{-1}A})\phi^k + \mathbf{B^{-1}}b \tag{30}
$$

The iteration is stable if $\|(\mathbf{I} - \mathbf{B^{-1}A})\| \leq 1$ and L_2 stability for a constant full-tensor is proven in [5]. The above iteration scheme converges with a specified tolerance. The flux-splitting formulations presented here are equally applicable to both structured and unstructured[5] control volume distributed formulations.

6 NUMERICAL RESULTS

In this section numerical results are presented with application of flux-splitting to the family of flux-continuous finite volume schemes. The matrix splitting methods presented in section 5 have been tested and the flux splitting scheme is found to yield the best performance (with fewer iterations) and is therefore used here. Flux-splitting techniques are also equally applicable to structured and unstructured grids.

6.1 Flux-splitting on structured grids

First we test the flux-splitting technique on a piecewise linear case where the exact solution is well known and monotonic. This example involves uniform flow over a rectangular domain. The medium is divided in two parts as shown in the figure 3(a). The grid
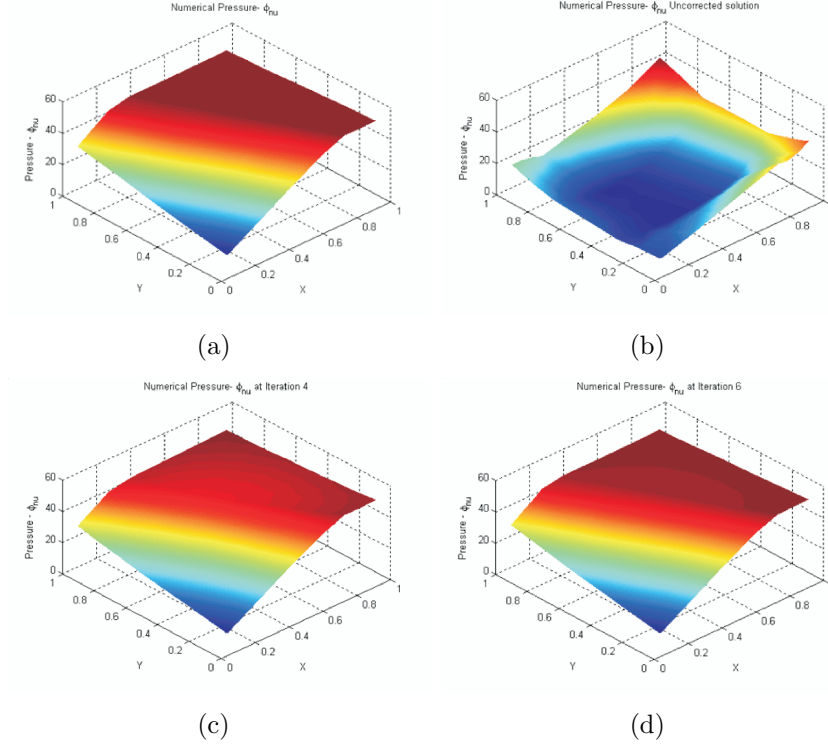
Figure 4: (a)Converged Solution. (b) Uncorrected Solution. (c) Solution after 4th iteration. (d) Solution after 6th iteration.

aligned along the discontinuity was used to obtain the numerical solution as shown in figure 3(b). The permeability field is discontinuous and permeability ratio is $1/100$ across the discontinuity. The analytical pressure is piece-wise linear and is given by

$$\phi(x,y) = \left\{ \begin{array}{ll} 200/3(x+y/2), & x+y/2 < 3/4, \\ 2/3(x+y/2)+99/2, & x+y/2 \geq 3/4, \end{array} \right. \tag{31}$$

A full discontinuous permeability tensor is defined as

$$K = \left\{ \begin{array}{ll} \left(\begin{array}{cc} 1 & -1/4 \\ -1/4 & 1/2 \end{array} \right), & x+y/3 < 3/4, \\ \left(\begin{array}{cc} 100 & -100/4 \\ -100/4 & 100/2 \end{array} \right), & x+y/2 \geq 3/4, \end{array} \right.$$

The flux-splitting technique presented in section 5.2 is used to obtain the numerical solution, figure 4. As the iteration proceeds the kth iterate is stored and solution at iteration $k+1$ is computed and tested for local extrema, if the test fails numerical solution at k^{th} iteration is selected otherwise solution at k^{th} iteration is overwritten with solution

obtained after $k+1$ iteration. Using this criteria it is possible to obtain a solution after 6th iteration with $O(h^3)$ error compared to the numerically converged solution, shown in figure 4(c) and figure 4(d).

Next we apply the method to a Green's function on a Cartesian grid, using the flux-splitting technique to obtain a monotonic solution for a case with high anisotropic ratio. The problem in consideration has a anisotropy ratio of 1/1000, with angle between grid and principal permeability axes is $\pi/6$ and thus violates Eq. 20. As with the direct discrete solution, the final converged solution is non-monotonic as shown in figure 5(a) because of high anisotropy and oscillations in numerical solution can be seen clearly in figure 5(b). Now, in order to obtain a monotonic solution the iteration proceeds unless a local extrema is detected. At each iterate a test for local extrema is conducted, away from sources and sinks, if for all nodes j connected to node i

$$min_j\phi_j \leq \phi_i \leq max_j\phi_j \tag{32}$$

the iteration proceeds, otherwise it is terminated before any non-monotonic behavior with spurious oscillations occurs. Thus the solution process is in effect non-linear. Further iteration strategies are currently being explored. The numerical results after the 7th and 20th iterations are presented for this case in figure 5(c) and 5(d) respectively. These non-converged solutions are monotonic and free from spurious oscillations as shown in solution contours (figure 5(d),5(e)) compared to the non-monotonic converged solution in figure 5(a).

Next we present a case with a source at $x = 0$ and $y = 0$ and a sink having the same strength but located at $x = a$ and $y = b$ is given as

$$\phi = \frac{Q}{2\pi}ln\frac{(x^2+y^2)^{1/2}}{[(x-a)^2+(y-b)^2]^{1/2}} \tag{33}$$

The analytical solution for the above equation along with numerical solution for a homogeneous diagonal permeability tensor is shown in figure 6(a) and 6(b). For a homogeneous diagonal permeability tensor the numerical solution obtained with flux-splitting is converging towards the analytical solution. However, for high anisotropy ratio the discrete finite volume approximation leads to an oscillatory solution as shown in figure 6(c) and 6(d) and hence loss of general monotonicity. Now on using the flux-splitting technique on this problem the results obtained after 6th and 14th iteration are shown in figure 7(a) and 7(b). It can be seen from the contour plots shown in figure 7(c) and 7(d) that the numerical solutions obtained are free of spurious oscillations and satisfy a general monotonicity condition.

6.2   Unstructured grids

The final test case involves applying the methods to a Green' function as before, now solved on an unstructured grid figure 8(a). The (direct method) discrete solution and
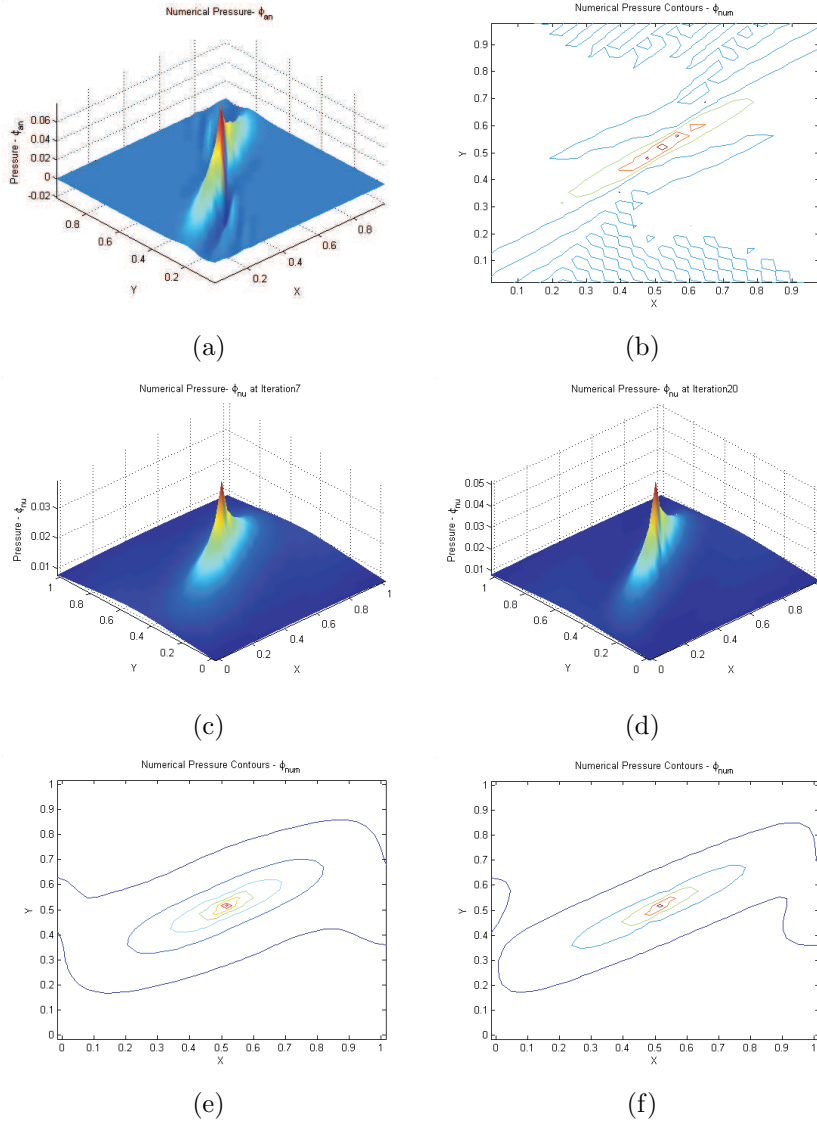
Figure 5: (a)Converged Solution of a Green's Function on anisotropic medium with anisotropic ratio of $1/1000$, angle between grid and principal permeability axes $\pi/6$. (b)Numerical solution contours showing the oscillations. (c) Solution after 7th iteration. (d) Solution after 20th iteration. (e)Oscillation free Numerical Pressure Contours after 7th iteration. (f)Oscillation free Numerical Pressure Contours after 20th iteration.

(a)　　　　　　　　　　　　(b)

(c)　　　　　　　　　　　　(d)
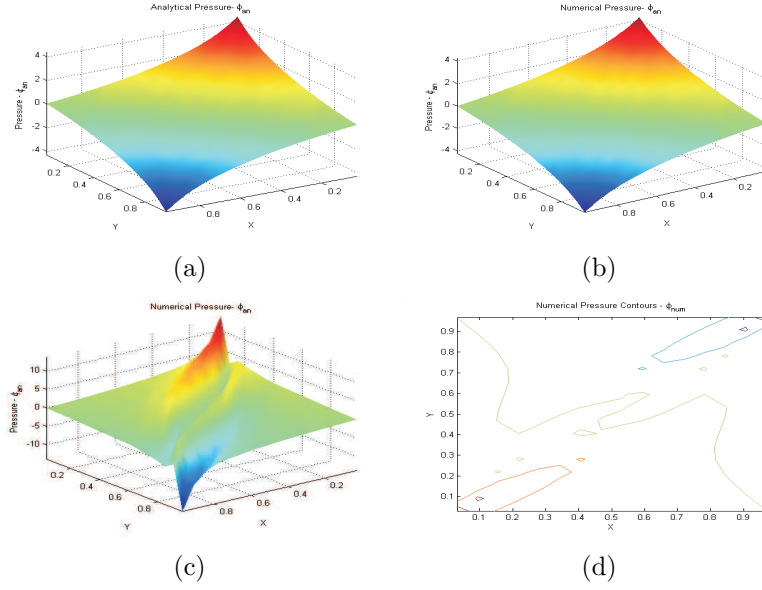
Figure 6: (a)Analytical solution for source and sink problem. (b)Numerical solution for source and sink problem with homogeneous diagonal permeability tensor. (c) Numerical solution for source and sink problem with high anisotropic medium with anisotropic ratio of $1/1000$, angle between grid and principal permeability axes $\pi/6$. (d)Numerical solution contours showing the oscillations.

(a)　　　　　　　　　　　　(b)

(c)　　　　　　　　　　　　(d)
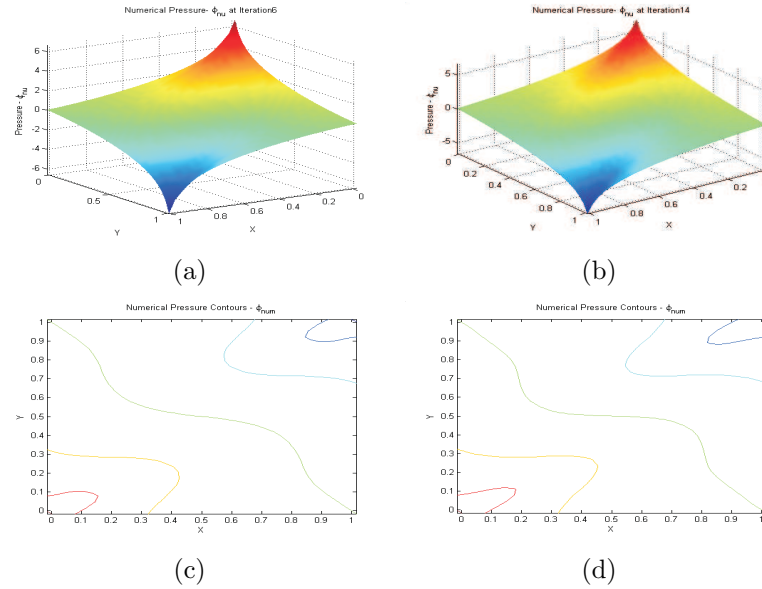
Figure 7: (a)Numerical Solution after 6th iteration. (b)Numerical Solution after 14th iteration.(c) Numerical Pressure contours after 6th iteration.(d)Numerical Pressure contours after 14th iteration.
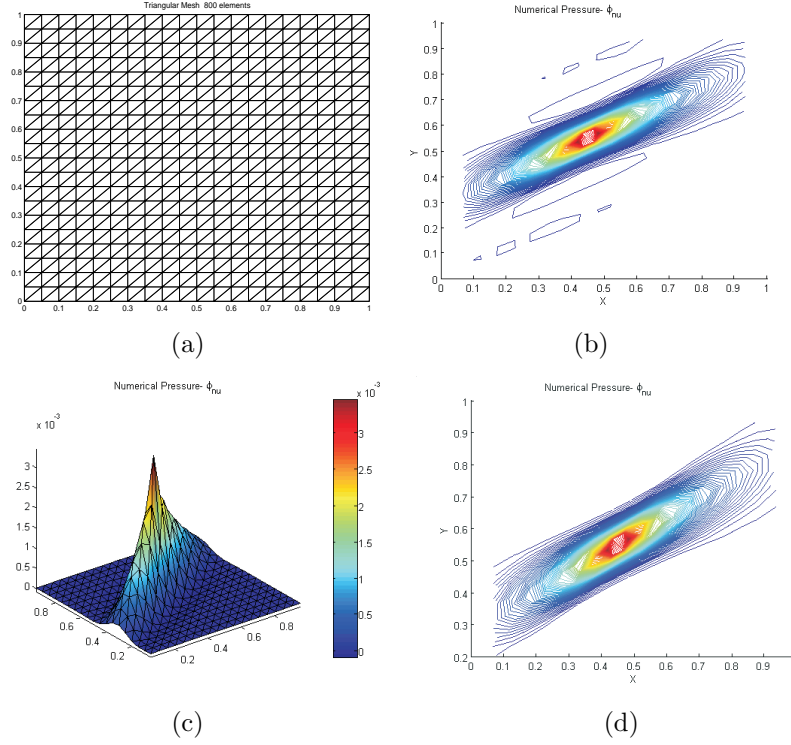
Figure 8: (a)Unstructured Mesh aligned with anisotropy. (b)Oscillatory Numerical Solution contours.(c)Oscillation free Numerical solution after 14th iteration.(d)Numerical Pressure contours after 14th iteration.

monotonic-split method solution are shown in figure 8(b), 8(c) and 8(d), which demonstrates the effectiveness of the method on unstructured grids.

6.2.1 Summary

A key component of this solution procedure is in obtaining a predicted monotonic solution computed by the two-point flux approximation, where the resulting M-matrix is used as a driver and the (deferred) correction to the iteration (in this case) is added at each iterative step until a local extrema is detected.

7 CONCLUSIONS

- In this paper two different kinds of splitting techniques are presented, which can be broadly classified into *Flux-splitting* and *Matrix-splitting*.
- The splitting techniques yield monotonic numerical solutions for full-tensor permeability fields with high principal anisotropy ratios.
- The flux-splitting technique is found to be most efficient as its convergence to final solution is faster compared to other splitting techniques. Flux-splitting also maintains

15

local conservation at any level of iteration.
- These splitting techniques are equally applicable to structured and unstructured grids in two and three dimensions.
- Splitting techniques may be more suitable for obtaining monotonic numerical solutions when compared to grid optimization, which appear to be applied at lower anisotropy ratio. The splitting technique is used here for anisotropy ratios of 1/1000 and higher.

8   ACKNOWLEDGEMENT

REFERENCES

[1] M.G.Edwards and C.F.Rogers, *Finite volume discretization with imposed flux continuity for the general tensor pressure equation.* Comput. Geo. (1998), no.2, 259-290.

[2] M.G.Edwards, *Unstructured, control-volume distributed, full-tensor finite volume schemes with flow based grids .* Comput.Geo. (2002), no.6, 433-452.

[3] M.G.Edwards, *Symmetric Positive Definite General Tensor Discretization Operator on Unstructured and Flow Based Grids.* 8th European Conference On Mathematics Of Oil Recovery,Freiberg, Germany, 3-6th September 2002.

[4] M.G.Edwards, *Control-volume distributed sub-cell flux schemes for unstructured and flow based grids.* SPE Reservoir Simulation Symposium, Hosuton, Texas, USA, 3-5 Febuary 2003.

[5] M.G.Edwards, *M-Matrix Flux Splitting for General Full Tensor Discretization Operators on Structured and Unstructured Grids.* Journal of Computational Physics 160, 1-28(2000).

[6] M.G.Edwards and M.Pal, *Symmetric Positive Definite General Tensor Discretization: A Family of Sub-cell Flux Continuous Schemes on Cell Centred Quadrilateral Grids.* Numerical Methods in Fluids (submitted).

[7] M. Pal, M.G.Edwards and A.R. Lamb, *Convergence study of a family of flux-continuous, Finite-volume schemes for the general tensor pressure equation.* Numerical Methods in Fluids (in press).

[8] M.Pal and M.G.Edwards, *Effective Upscaling Using a Family of Flux-Continuous, Finite-Volume Schemes for the Pressure equation.* In Proceedings, ACME Conference, Queens University Belfast($19 - 20^{th} April, 2006$).

[9] I.Aavatsmark,T.Barkve,Ø.Bøe, and T.Mannseth, *Discretization on non-orthogonal, quadrilateral grids for inhomogeneous, anisotropic media.* J.Comput.Phys.(1996),no.127,2-14.

[10] I.Aavatsmark, T.Barkve,Ø.Bøe, and T.Mannseth. *Discretization on unstructured grids for inhomogeneous, anisotropic media. Part I: Derivation of the methods.* SIAM J.Sci.Comput.(1998),no.19,1700-1716.

[11] I.Aavatsmark, T.Barkve,Ø.Bøe, and T.Mannseth. *Discretization on unstructured grids for inhomogeneous, anisotropic media. Part II: Discussion and numerical results.* SIAM J.Sci.Comput.(1998),no.19,1717-1736.

[12] I.Aavatsmark, *Introduction to multipoint flux approximation for quadrilateral grids.* Comput.Geo(2002),no.6,405-432.

[13] G.T.Eigestad, I.Aavatsmark, M.Espedal, *Symmetry and M-Matrix issues for the O-method on an unstructured grid.* Computational Geo Sciences. 6, 381-404 (2002).

[14] S. H. Lee, H.Tchelepi and L. J. DeChant, *Implementation of a Flux Continuous Finite Difference Method for Stratigraphic Hexahedron Grids* paper SPE 51901 proc: SPE Reservoir Simulation Symposium, Houston, Texas, USA Feb 14th - 17th 1999

[15] S.H.Lee, P.Jenny, H.A.Tchelepi, *A finite-volume method with hexahedral multiblock grids for modeling flow in porous media.* Comput.Geo(2002),no.6,353-379.

[16] S.Verma, *Flexible grids for reservoir simulation.* Ph.D.thesis, Stanford University (June 1996).

[17] L.J.Durlofsky, *A triangle based mixed finite element finite volume technique for modeling two phase flow through porous media.* J.Comput.Phys(1993),252-266.

[18] B.Riviere, *Discontinuous Galerkin method for solving the miscible displacement problem in porous media.* Ph.D.thesis, The University of Texas at Austin,(2000).

[19] B.Riviere, M.F.Wheeler, K.Banas, *Discontinuous Glaerkin method applied to a single phase flow in porous media.* Comput.Geo(2000),no.49,337-3.

[20] T.F. Russel and M.F. Wheeler, *Finite Element and Finite Difference Methods for Continuous Flows in Porous Media.* Chapt 2, in the Mathematics of Reservoir Simulation, R.E. Ewing ed, Frontiers in Applied Mathematics SIAM 1983, pp 35 -106

[21] T. Aadland, I. Aavatsmark and H.K. Dahle, *Performance of a flux splitting when solving the single-phase pressure equation discretized by MPFA*. Comput.Geo,Volume 8, Number 4, December 2004, pp. 325-340(16)

[22] J.M.Nordbotten and G.T.Eigestad, *Discretization on quadrilateral grids with improved monotonicity properties*,Journal of Computational Physics 203(2), 744-760, 2005.

[23] J.M.Nordbotten and I.Aavatsmark,*Monotonoicity conditions for control volume methods on uniform parallelogram grids in homogeneous media.* Computational Geosciences, Volume 9 (2005), 61-72.

[24] Martin J. Mlacnik and Louis J. Durlofsky *Unstructured Grid Optimization for Improved Monotonocity of Discrete Solutions of Elliptic Equation with Highly Anisotropic Coefficients* Submitted to Elsevier Science.

[25] O. Axelsson, *Iterative Solution Methods*, Cambridge University Press, Cambridge 1994.